Environmental Science & Technology

pubs.acs.org/est

Article

Aerobic Degradation of the Antidiabetic Drug Metformin by *Aminobacter* sp. Strain NyZ550

Tao Li, Zhi-Jing Xu, and Ning-Yi Zhou*

Cite This: *Environ. Sci. Technol.* 2023, 57, 1510−1519

Read Online

ACCESS | Metrics & More | Article Recommendations | Supporting Information

ABSTRACT: Metformin is becoming one of the most common emerging contaminants in surface and wastewater. Its biodegradation generally leads to the accumulation of guanylurea in the environment, but the microorganisms and mechanisms involved in this process remain elusive. Here, *Aminobacter* sp. strain NyZ550 was isolated and characterized for its ability to grow on metformin as a sole source of carbon, nitrogen, and energy under oxic conditions. This isolate also assimilated a variety of nitrogenous compounds, including dimethylamine. Hydrolysis of metformin by strain NyZ550 was accompanied by a stoichiometric accumulation of guanylurea as a dead-end product. Based on ion chromatography, gas chromatography−mass spectrometry, and comparative transcriptomic analyses, dimethylamine was identified as an additional hydrolytic product supporting the growth of the strain. Notably, a microbial mixture consisting of strain NyZ550 and an engineered *Pseudomonas putida* PaW340 expressing a guanylurea hydrolase was constructed for complete elimination of metformin and its persistent product guanylurea. Overall, our results not only provide new insights into the metformin biodegradation pathway, leading to the commonly observed accumulation of guanylurea in the environment, but also open doors for the complete degradation of the new pollutant metformin.

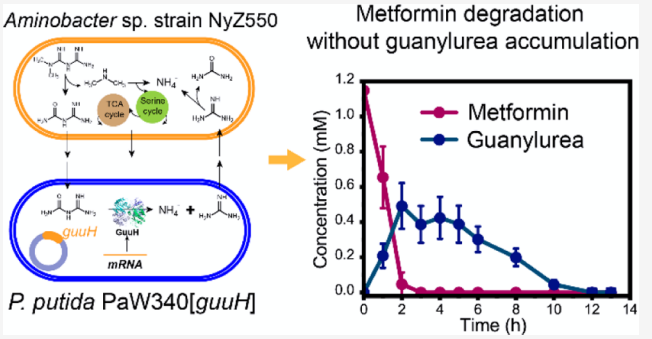

KEYWORDS: *bacteria, biodegradation, emerging contaminant, guanylurea, metformin*

1. INTRODUCTION

Pharmaceuticals in the environment are considered emerging contaminants and are of global concern due to their gradually revealed risks to ecosystems and human health.[1] Pharmaceutical pollution is primarily due to the use of pharmaceuticals by humans or animals, resulting in their continuous release into the environment through wastewater treatment plants (WWTPs) worldwide.[2] Most pharmaceuticals are synthetic compounds or natural products with modifications, affecting biological targets even at extremely low concentrations. Their presence in the environment has adverse effects on the ecosystems, aquatic organisms, and humans.[3,4] However, these effects are largely underestimated due to the lack of comprehensive data on their unpredictable synergistic toxicity and the risks of their structurally diverse products, as well as on the biodegradability[5] and environmental fate of pharmaceuticals.[1]

Metformin (MET) (1,2-dimethylbiguanide) is a synthetic guanidine derivative used as a blood glucose-lowering drug for type II diabetes. Currently, more than 500 million people worldwide have diabetes, primarily type II diabetes, with the number estimated to increase to 783 million by 2045.[6] Due to the worldwide prevalence of diabetes and the need for long-term medication, MET has become one of the most commonly used prescription drugs.[7] However, MET is not metabolized by the human body and is excreted as a prototype in urine and feces after oral administration.[8,9] Therefore, most MET will converge on WWTPs, leading to high concentrations of MET in the wastewater of WWTPs, with concentrations up to 702 μg L^{-1} observed in United States.[10] During flow through the WWTPs, MET is mainly transformed by biological processes. The present treatment of WWTPs shows incomplete elimination of MET with removal rates ranging from 41% to more than 98%, and ultimately significant amount of MET from WWTPs is released into the environment.[11] Consequently, the worldwide occurrence of MET has been observed in surface, ground, drinking and coastal waters, sludges, and soils.[2,10,12,13] It has recently been categorized as one of the top pharmaceuticals present in the environment.[2,14] MET exposure exhibits adverse effects on aquatic life[15−17] and can accumulate in plants.[18] In addition, its transformation

Received: October 18, 2022
Revised: December 23, 2022
Accepted: December 31, 2022
Published: January 9, 2023

products such as guanylurea (GUA)[19,20] and chlorination byproducts,[21] appear to be toxic and widely distributed.[12,22−26]

The widespread occurrence and obvious risks of MET and its derivatives necessitate remediation of MET-contaminated environments. Developing biodegradation technologies compatible with current wastewater treatment processes is considered a cost-effective and promising strategy. However, this is limited by a lack of available MET-degrading bacterial strains and knowledge of their degradative properties. Microbial consortia from soils or activated sewage sludge have been demonstrated to be able to degrade MET and GUA under aerobic or anaerobic conditions.[19,20,27−31] It has been suggested that aerobic conditions are preferred for MET degradation, whereas GUA degradation is faster under anaerobic conditions.[29] However, aerobic degradation of GUA was promoted by the addition of glucose as a co-substrate, suggesting that GUA can be readily used as a sole nitrogen source.[30] *Pseudomonas mendocina* GU was recently isolated from WWTPs for its ability to grow on GUA as a sole nitrogen source.[32] A novel hydrolase was identified that catalyzed the initial hydrolysis of GUA, and the resulting ammonium and guanidine were assimilated by this strain. Till date, only a single bacterial strain (*Aminobacter* sp.) capable of using MET as the sole carbon source has been isolated from activated sludge, and the strain converts MET into the dead-end product GUA, but further details of this degradation have not been investigated.[31]

In this study, we determined the concentrations of MET and GUA in wastewater from 12 WWTPs in China and the MET-degrading capacity of microbial consortia from these samples. The results helped us successfully isolate a MET utilizer, the *Aminobacter* sp. strain NyZ550, capable of growing on MET as a sole source of carbon, nitrogen, and energy. An investigation of the degradation of MET by strain NyZ550 revealed the following characteristics: (i) strain NyZ550 has a robust ability to degrade MET, (ii) strain NyZ550 is a versatile metabolizer of nitrogen-containing compounds, and (iii) the degradation of MET produces GUA and dimethylamine (DMA) via hydrolysis, with the former a dead-end product and the latter supporting the growth of strain NyZ550. Consequently, a microbial mixture composed of strain NyZ550 and an engineered *Pseudomonas putida* PaW340 expressing GUA hydrolase exhibits a capacity for both MET and GUA degradation.

2. MATERIALS AND METHODS

2.1. Reagents. MET (1,1-dimethylbiguanide hydrochloride), guanylurea sulfate salt hydrate, and dicyandiamide were purchased from TCI (Shanghai, China). Methylamine, DMA (40% in water), trimethylamine (30% in water), and water-^{18}O were purchased from Sigma-Aldrich (St. Louis, USA). Guanidine and 1,1-dimethylguanidine were purchased from YuanYe Bio-Technology (Shanghai, China). Biuret, 1-methylbiguanide, and biguanide were purchased from Bidepharm (Shanghai, China). All chemicals had a purity of >97%. Other commercial inorganic chemicals of analytical grade were used in this study. Ultrapure water and HPLC grade methanol were used to prepare the samples and mobile phases for ultra-performance liquid chromatography (UPLC).

2.2. Wastewater Sample Collection. Wastewater samples were collected from domestic WWTPs from 11 cities in China in April 2021. Each WWTPs had a treatment capacity of 85,000−200,000 m^3 per day, and all of them had an aeration tank where the wastewater was sampled. Biodegradability tests were conducted within 1 week after the samples were transported to the laboratory. For LC−MS analyses, 10 mL of each sample was pretreated by direct filtration with 0.22 μm nylon filters. Filtered samples were adjusted to pH 7.0 with 1 M NaOH or HCl and stored at −20 °C.

2.3. Batch Cultures. Batch experiments to test the biodegradability of the wastewater samples toward MET were performed in 250 mL Erlenmeyer flasks sealed with the polytetrafluoroethylene ventilatory film (pore diameter 0.2−0.3 μm). The flasks containing 100 mL of minimal salt medium (MSM, pH 7.0)[33] and 1.5 mM MET were added with an appropriate volume of the wastewater sample as inoculum to a density of approx. 10^4 to 10^5 colony forming units (CFUs) per mL, determined by serial dilution of wastewater and plate count of microorganisms grown on the Tryptic Soy Broth agar plate. The cultures were incubated at 30 °C in a shaking incubator at 180 rpm. Samples were taken at appropriate intervals in triplicate for measuring the concentrations of MET in the cultures. The cultures were transferred to new flasks after 12 days of incubation. An equal volume of autoclaved wastewater was inoculated as a control.

2.4. Isolation and Growth of MET-Utilizing Microorganisms. The batch cultures capable of degrading MET were used for further enrichment and isolation of MET utilizers according to a method previously described.[33] The pure isolates were identified by amplifying and sequencing the 16S rRNA gene sequences using primers 27F (5′-AGAGTTTGATCCTGGCTCAG-3′) and 1492R (5′-TACGACTTAACCCCAATCGC-3′). The isolates were grown in MSM containing MET or other substrates with indicated concentrations (1−8 mM) at 30 °C. Medium was supplemented with 0.2% (w/v) ammonium sulfate as a nitrogen source or 10 mM glucose as a carbon source if necessary. The population doubling time was estimated as a method previously described.[34] The optimal growth conditions of the MET utilizer were tested by culturing the strain in MSM containing 2 mM of MET under various pH, temperature, and salinity conditions. The pH values were adjusted by phosphoric acid or 1 M sodium hydroxide.

2.5. Isotope Labeling Experiment. MET was dissolved in $H_2{}^{18}O$ or H_2O at a concentration of 0.1 M as the stock standard. The MET utilizer NyZ550 was inoculated into 150 mL of MSM containing 2 mM MET and grown to the late exponential phase ($OD_{600\ nm}$ of approx. 0.04) at 30 °C. Then, cells were harvested by centrifugation (7000×*g*, 10 min, 4 °C) and washed twice with 50 mM Tris−HCl buffer (pH 8.0). The cells were divided into two equal volumes, one of which was incubated with 500 μM MET dissolved in $H_2{}^{18}O$ and the other with 500 μM MET dissolved in H_2O. The reaction mixtures were incubated at 30 °C for 1 h and the products were analyzed by UPLC-QTOF MS. All reactions were performed in triplicate.

2.6. Enzyme Assays. Strain NyZ550 was grown on MET and harvested as described above. The pellet was suspended in MSM and then lysed by sonication. The resulting cell lysate was centrifuged at 16,000×*g* for 40 min to remove debris, and the supernatant was used for enzyme assays. The reaction mixtures (0.5 mL) containing 500 μg of protein from the crude extract and 0.5−1 mM MET in 50 mM Tris−HCl buffer (pH 8.0) were incubated at 30 °C. Samples were removed at appropriate intervals and analyzed by UPLC-QTOF MS, gas chromatography−MS (GC−MS), and ion chromatography.

https://doi.org/10.1021/acs.est.2c07669
Environ. Sci. Technol. 2023, 57, 1510−1519

The spectrum change during the reaction was recorded using a Lambda 25 spectrophotometer (PerkinElmer/Cetus, Norwalk, CT).

2.7. Analytical Methods. MET and GUA were quantified using an UPLC system (Agilent 1260 Infinity II) connected in series with triple quadrupole mass spectrometry (TQMS/MS, Agilent 6470 system). The UPLC system was equipped with an XBridge phenyl column (3.5 μm × 150 mm × 2.1 mm). Mobile phase A was ultrapure water containing 10 mM ammonium formate (adjusted to pH 3.5 with formic acid), and mobile phase B was methanol. The UPLC gradient started at 5% B, which was held for 4.5 min, then increased to 95% at 8.5 min, where it remained until 9 min, and was then reduced to 5% at 15 min before a 5 min re-equilibration. The binary mobile phase was set to a flow rate of 0.2 or 0.4 mL/min, and the injection volume was 10 μL. For MS analysis, electrospray ionization was used to generate two transition ions from analytes in the positive ionization mode, one transition ion for quantification and the other for confirmation. The following ion transitions (m/z) were used: MET 130/60 and 130/73, GUA 103/60 and 103/43. The ionization parameters were set as follows: the desolvation gas temperature was 320 °C, the drying gas flow was 8 L/min, the nebulizer pressure was 35 psi, the capillary voltage was 4 kV, and the collision energy was 20 eV. Quantification was achieved using the external standard method and Agilent MassHunter Quantitative Analysis software (version B.08.00). The calibration curves were generated by calculating the peak area versus the concentration of each target compound (Table S1). The limits of detection were 10 and 15 ng/L for MET and GUA, respectively.

The Agilent 1290 Infinity II-Agilent 6545 QTOF MS system was used for qualitative analyses of GUA and other compounds, as indicated. The LC system was operated as described above, and QTOF MS was performed using an electrospray source in the positive mode with a mass range of 50−500 m/z. The ionization parameters were set as following: the desolvation gas temperature was 300 °C, the drying gas flow was 5 L/min, the nebulizer pressure was 45 psi, and the capillary voltage was 4 kV.

DMA was analyzed with an ICS-900 ion chromatograph (Thermo Fisher Scientific, CA, USA) composed of a dual-piston pulse infusion pump system, eluent generator, and digital conductivity detector. The separation was performed by a Dionex IonPac C16 column (5 × 150 mm) maintained at 30 °C and a conductivity detector using an external calibration. The eluent solution contained 10 mM methanesulfonic acid at a flow rate of 1 mL/min for 50 min. The injection volume was 25 μL. In addition, DMA was also identified using a GC−MS QP2010 SE system (Shimadzu Corporation, Japan) in the SIM mode under the following conditions: an SH-I-5MS column (30 m × 0.25 μm × 0.25 mm) was used and interface and source temperatures were 220 °C. The oven temperature procedure was 50 °C for 1 min, increased to 160 °C at 10 °C/min, held for 1 min, then increased to 300 °C at 20 °C/min.

2.8. Genome and Transcriptome Sequencing. The MET-grown NyZ550 cells were collected, as described above, and their genomic DNA was extracted by an UltraClean Microbial DNA Isolation kit (MoBio Laboratories, Inc., USA). The total DNA of NyZ550 was sequenced by an Illumina HiSeq platform with the paired-end mode. The sequenced reads were assembled using SOAPdenovo2 software.[35] The draft genome sequence of strain NyZ550 was deposited in the NCBI database under the project PRJNA882228.

Strain NyZ550 cells grown on glucose (GLU group) or MET (MET group) were collected and sent to the Personalbio Technology Co., Ltd. (Shanghai, China) for RNA sequencing. Total RNA was extracted using a TRIzol-based method (Life Technologies, CA), resulting in RNA samples with a concentration of more than 250 ng/μL. Then, RNA libraries of 300−400 bp were constructed and sequenced by the Illumina platform. The adapter sequences and low-quality reads from the raw data were removed before gene expression analysis. The gene expression levels were evaluated as fragments per kilobase of transcript per million fragments (FPKM). The fold change of gene expression was calculated by comparison of the FPKM values of the MET group to those of the GLU group. The differentially expressed genes (DEGs) were identified by a $|\log_2$ foldchangel >1 (p-value < 0.05). The transcriptomic raw data were deposited to the NCBI database with accession numbers SRR22556978 and SRR22556977.

2.9. Degradation of MET by a Microbial Mixture. The GUA hydrolase gene (*guuh*, GenBank accession number: MBF8163004.1) was synthesized by Tsingke Biotechnology (Shanghai, China). The *guuh* gene was amplified by the primers *guuh*-S (5′-GACGGCCAGTGAATTTCAGGCT-GAAGCCAGCG-3′) and *guuh*-A (5′-TGATTACGC-CAAGCTTCGAAAGGTTTTGCACCATTCGATGG-3′) and then inserted into the pRK415 vector by homologous recombination. The *guuh* was expressed under the control of a *tac* promoter. The construct pRK415-*guuh* was then introduced into *P. putida* PaW340 by electrotransformation, as described previously.[36] Strain PaW340 carrying pRK415-*guuh* was grown in 150 mL of LB medium containing 10 μg/mL tetracycline at 30 °C to an optical density at 600 nm ($OD_{600\ nm}$) of 0.3. *Aminobacter* sp. strain NyZ550 was grown in 150 mL of MSM containing 2 mM MET to the exponential phase. The two cultures were harvested by centrifugation and washed twice with 50 mM Tris−HCl (pH 8.0) and resuspended in MSM to a density of 3.2 × 10^8 cells/mL. The PaW340 cell suspension was divided into two parts, with one part was used for biotransformation of GUA and the other mixed with equal number of NyZ550 cells (approx. 6.4 × 10^9 cells in total), which was used as a microbial mixture for biotransformation of MET. The biotransformation mixtures were incubated in a shaker at 220 rpm, 30 °C. Samples were removed at appropriate intervals and analyzed using UPLC-MS/MS. Control experiments were performed using PaW340 cells carrying the empty pRK415 vector. All the assays were tested in triplicate.

3. RESULTS AND DISCUSSION

3.1. MET and GUA Were Prevalent in Samples from WWTPs in China. The concentrations of MET and GUA in 12 wastewater samples were measured by UPLC-TQMS/MS. As shown in Table 1, MET was detected in all samples with a large variation in concentrations, ranging from 0.1 to 486.5 μg L^{-1}. GUA, a known metabolite of MET, was detected in 9 of the 12 samples with concentrations ranging from 202.6 to 686.5 μg L^{-1}. The levels of MET and GUA in each environmental sample exhibited a negative correlation. In the nine samples with high GUA concentrations, the concentrations of MET were merely in the range of 0.1−31.8 μg L^{-1}, while the remaining three samples (WX, NJ2, and SJZ) in which GUA was not detected had high MET concentrations (247.2−486.5 μg L^{-1}). This result is consistent with previous observations in samples from WWTPs[24] and is likely due to

https://doi.org/10.1021/acs.est.2c07669
Environ. Sci. Technol. 2023, 57, 1510−1519

Table 1. Concentrations of MET and GUA in the Wastewater of Municipal WWTPs from 11 Cities in China[a]

sites	concentrations (μg/L)[b]	
	MET	GUA
Beijing (BJ)	31.77 ± 0.41	265.06 ± 67.01
Changzhou (CZ)	0.90 ± 0.05	202.61 ± 14.24
Guangzhou (GZ)	0.11 ± 0.01	495.41 ± 145.88
Hangzhou (HZ)	0.19 ± 0.03	388.67 ± 148.58
Lanzhou (LZ)	1.32 ± 0.34	589.59 ± 229.05
Nanjing1 (NJ1)	5.05 ± 0.46	397.4 ± 61.29
Nanjing2 (NJ2)	247.2 ± 42.84	ND
Shanghai (SH)	3.37 ± 0.53	373.93 ± 122.83
Shijiazhuang (SJZ)	320.54 ± 12.15	ND
Wuxi (WX)	486.52 ± 77.67	ND
Xiamen (XM)	1.14 ± 0.03	686.5 ± 131.38
Yuhang (YH)	1.24 ± 0.04	288.14 ± 97.39

[a]ND: not detected. [b]The data shown are average values of replicate samples (n = 3).

the distinct ability of microorganisms to convert MET into GUA in wastewater.

3.2. Distinct MET-Degrading Capacity of Indigenous Microorganisms from Wastewater. To compare the MET-degrading abilities of indigenous microorganisms from different wastewater samples, batch culture biodegradation tests were performed. MSM containing MET (from 0.9 to 1.5 mM) was inoculated with wastewater from different WWTPs, and MET concentrations were measured over time (Figure 1). Almost complete degradation of MET was observed in nine cultures within 10 days, whereas three cultures (WX, NJ2, and SJZ) showed a poor capacity to degrade MET within 12 days. Interestingly, these three cultures were derived from the three original samples in which GUA was not detected but had high concentrations of MET (WX, NJ2, and SJZ, as listed in Table 1). The 12 cultures were further transferred after 12 days to fresh media with 1% (v/v) inoculum and cultured under the same conditions. Similar degradation behaviors were observed in the second transfers as in the first ones, except for sample SJZ, which showed a complete degradation of MET but over a longer period (12 days), indicating a possible microbial adaption or evolution for MET degradation. Cultures WX and NJ2 were still unable to degrade MET even after extending the culturing period to 26 days. No evident elimination of MET was observed in the controls of the autoclaved wastewater samples, indicating that MET was not transformed through an abiotic manner under the conditions used.

3.3. MET-Utilizing Bacteria Were Isolated from WWTPs. After selective enrichment on MET of the cultures exhibiting MET degrading capacity, five phylogenetically related *Aminobacter* sp. strains with the ability to grow on MET were obtained from different samples, and their 16S rRNA gene sequences were deposited in GenBank (Table S2). These strains exhibited a similar degradation behavior for MET, and therefore, an isolate from sample SH (designated *Aminobacter* sp strain NyZ550) was used for further analyses.

Strain NyZ550 was shown to almost completely degrade (99.8 ± 0.14%) MET within 60 h with an increase in cell biomass (Figure 2). No degradation of MET was observed in the control without inoculation of strain NyZ550, and no growth was observed in the control without the addition of MET (Figure 2). The results clearly established that the MET loss was due to biodegradation by strain NyZ550. The strain grew well at temperatures of 15−30 °C, preferred neutral or alkaline conditions (pH 6.0−10.0), and tolerated salinity up to 2% (as NaCl, w/v %) (Figure S1).

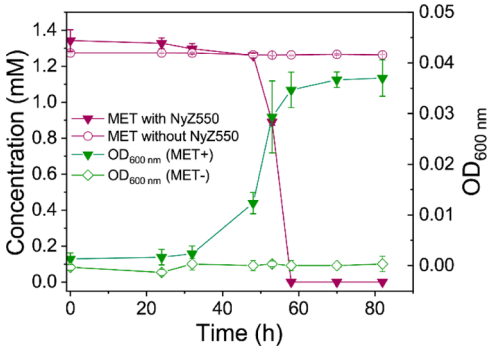

Figure 2. Growth of *Aminobacter* sp. strain NyZ550 on MET (MET$^+$) as a sole source of carbon, nitrogen, and energy. Controls were conducted without inoculation or without addition of MET (MET$^-$). Growth (green lines) is indicated by the increased optical density at 600 nm ($OD_{600\ nm}$), and the concentrations of MET are shown in fuchsia lines.

3.4. Strain NyZ550 Grows on a Variety of Nitrogenous Substrates. Nitrogen availability is often a growth-limiting factor for bacteria, and strains of *Aminobacter* are known for their versatile abilities to utilize nitrogenous compounds, thereby conferring them a selective advantage in the environment.[37,38] Here, we tested the growth of strain NyZ550 on various nitrogenous compounds (2 mM) analogous to MET or derived from MET. The results showed

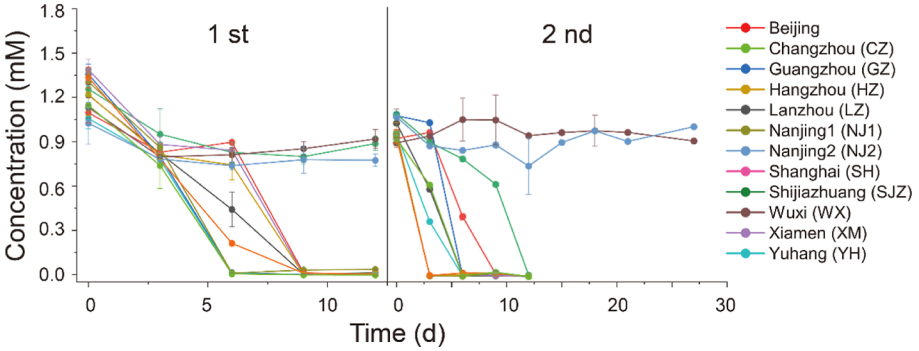

Figure 1. MET degrading capacity of the microbial consortia from wastewater of 12 WWTPs in China. The first transfer (first) and second transfer (second) were performed in minimal salt media containing MET.

https://doi.org/10.1021/acs.est.2c07669
Environ. Sci. Technol. 2023, 57, 1510−1519

that strain NyZ550 was able to use trimethylamine, DMA, methylamine, and 1-methylbiguanide as sole carbon, nitrogen, and energy sources for its growth (Figures 3A and S2). The

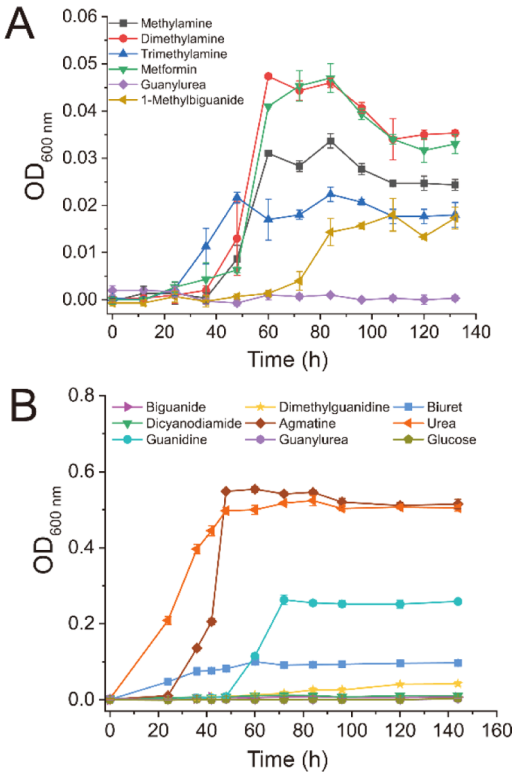

Figure 3. Growth of *Aminobacter* sp. strain NyZ550 on a variety of nitrogenous compounds. The structures of these compounds can be found in Figure S3. (A) Compounds (2 mM each) indicated were used as the sole source of carbon and nitrogen. (B) Compounds (2 mM each) indicated were used as the sole source of nitrogen, and 10 mM glucose was used as the carbon source.

doubling time of strain NyZ550 grown on these substrates was 10.2 ± 1.3, 4.8 ± 0.2, 6.6 ± 1.5, and 8.5 ± 1.5 h, respectively. The low biomass yields could be due to the inefficiency in transportation, un-optimized catabolic flux, or toxicity caused by the substrates. Other nitrogenous compounds, including guanidine, biuret, urea, and agmatine, could only be used as the sole nitrogen source for growth by strain NyZ550 (Figure 3B). However, no clear growth was observed using biguanide, dicyandiamide, or the MET degradation product GUA under the same culture conditions.

3.5. Identification of the Catabolic Product GUA. Considering the extremely high proportion of GUA versus MET in the sample SH, from which strain NyZ550 was isolated, it was assumed that GUA was a degradation metabolite. Therefore, identification of metabolites produced during growth of strain NyZ550 on MET was performed using UPLC-QTOF MS. A product peak with a retention time of 8.9 min was confirmed to be GUA based on comparison of the retention time and mass spectra ($[M + H]^+$: 103.0616, mass accuracy: 1.94 parts per million [ppm] error) with those of authentic GUA (Figure S4). During the growth of strain NyZ550, a stoichiometric accumulation of GUA was observed in the culture with the disappearance of MET, but GUA was not further degraded, even after culturing for an extended period after MET was transformed (Figure 4A). Moreover, strain NyZ550 was unable to grow on GUA with or without the addition of glucose, indicating that GUA could not be used as the source of carbon or nitrogen for growth (Figure 3). These observations established that GUA was a dead-end product in MET degradation by strain NyZ550. This may well explain the accumulation of GUA in the wastewater (sample SH) from which the strain NyZ550 was isolated. This same catabolic process is likely to be present in other samples with high GUA concentrations in this study.

3.6. Incorporation of the ^{18}O Atom of $H_2{}^{18}O$ into GUA during MET Degradation. To determine the source of the oxygen atom incorporated into GUA and the reaction type for the formation of GUA from MET degradation, biotransformation assay was performed to convert MET into GUA by strain NyZ550 in $H_2{}^{18}O$, and the product was examined by mass spectrometry. The molecular ion of ^{18}O atom-labeled GUA (m/z 105) appeared at a position two mass numbers higher than the corresponding ion of unlabeled GUA (m/z 103) (Figure S5). The observed product ratio of ^{18}O labeled and unlabeled GUA was about 20: 1, and this is likely because of the incorporation of H_2O within the cells. The result indicated that the ^{18}O atom of $H_2{}^{18}O$ was incorporated into the GUA, thus clarifying that the reaction proceeded via hydrolysis.

3.7. Identification of DMA as Another Initial Degradation Product. The evidence above dictates the biodegradation of MET by NyZ550 with the accumulation of

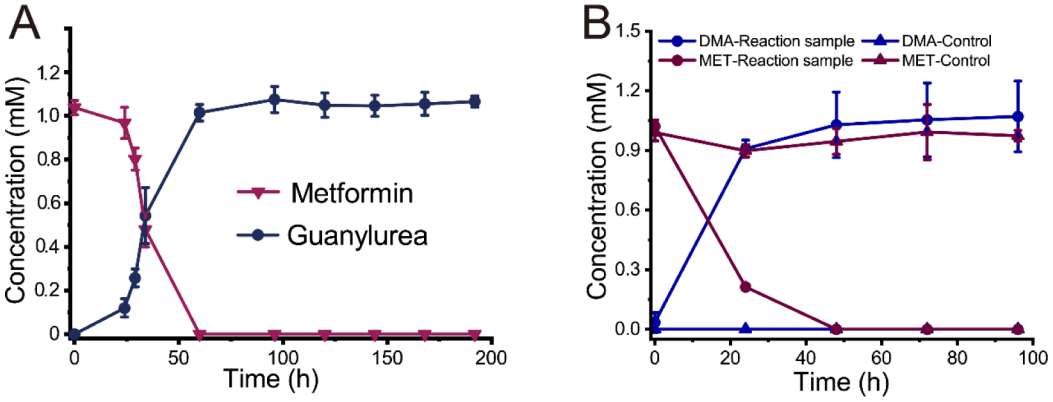

Figure 4. Identification of the MET degradation products GUA and DMA. (A) Quantification of GUA formation along with the degradation of MET during the growth of strain NyZ550. (B) Quantification of DMA formation along with the degradation of MET in crude enzyme assays. The reaction mixture contained Tris−HCl buffer (pH 8.0), 1 mM MET, and 0.5 mg of crude enzyme prepared from MET-grown NyZ550 cells.

https://doi.org/10.1021/acs.est.2c07669
Environ. Sci. Technol. 2023, 57, 1510−1519

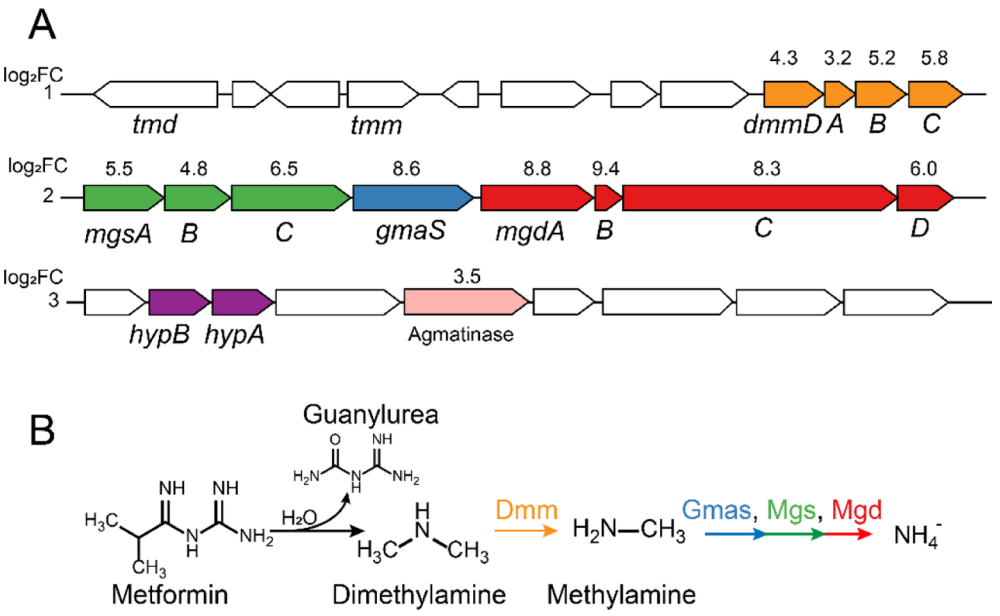

Figure 5. Proposed MET degradation pathway and involved genes in *Aminobacter* sp. strain NyZ550. (A) Gene clusters involved in catabolism of MET. The transcriptional levels of genes in the MET degradation pathway are upregulated, as indicated by the $\log_2$ foldchange values upon each gene. FC, foldchange. Clusters 1 and 2 encompass the methylamine catabolic genes. Tmm, trimethylamine monooxygenase; Tdm, trimethylamine *N*-oxide demethylase; *DmmABC*, DMA monooxygenase; Gmas, γ-glutamylmethylamide synthetase; MgsABC, *N*-methylglutamate synthase; and MgdABCD, *N*-methylglutamate dehydrogenase. Cluster 3 contains the genes encoding the nickel incorporation proteins (HypAB) and agmatinase. (B) Proposed MET degradation pathway in strain NyZ550.

the dead-end product GUA, but the exact intermediates for supporting the growth of NyZ550 are unknown. Two possible pathways for bacterial transformation of MET to GUA were proposed (Figure S6). One was initialized by demethylation, with the intermediates including 1-methylbiguanide and biguanide. Although 1-methylbiguanide was previously detected in batch experiments with activated sludge from WWTPs,[29] in this study, it was not observed in growth or biotransformation assays when compared to standard in LC-QTOF MS analysis. Another possible pathway was the direct hydrolysis of MET with the probable release of DMA. Therefore, we performed an enzymatic assay to detect DMA using the crude enzyme prepared from MET-grown NyZ550 cells. The activity of the crude enzyme on MET was confirmed by the decrease in the characteristic absorption of MET at 233 nm during the enzymatic reaction (Figure S7A,B), as well as the formation of product GUA in the reaction mixture (Figure S7C,D). Most importantly, a significant amount of DMA was detected in the reaction mixtures by ion chromatography (Figure S8) and GC−MS (Figure S9). Consumption of 1.02 ± 0.03 mM MET led to the formation of 1.12 ± 0.18 mM DMA in the reaction mixture within 72 h (Figure 4B). DMA was a favorable growth substrate for strain NyZ550 but GUA was not (Figure 3). Furthermore, we observed that an equivalent amount of DMA and MET resulted in an equal biomass accumulation of strain NyZ550 (Figure S10), indicating that DMA was the only intermediate supporting bacterial growth.

3.8. Genes Involved in MET Degradation in Strain NyZ550. To further elucidate the degradation mechanism of MET by strain NyZ550, complete genome and comparative transcriptome analyses were carried out to identify the DEGs in response to MET. A total of 5883 expressed genes were detected, and of them, 107 genes were upregulated, and 104 genes were downregulated (Figure S11A). KEGG analysis showed that the upregulated genes were significantly enriched ($p < 0.01$) in pathways of photosynthesis, flagellar assembly, ribosome, glyoxylate and dicarboxylate metabolism, methane metabolism, one-carbon pool by folate, and glycine, serine, and threonine metabolism (Figure S11B). In addition, GO annotation analysis also showed that the upregulated genes were enriched in the tricarboxylic acid cycle and one-carbon metabolism, implying that these processes were likely to participate in MET degradation.

3.8.1. Genes Involved in the MET Degradation Pathway of Strain NyZ550. Based on the genomic annotation, there were two gene clusters in the genome of strain NyZ550 encoding the methylamines degradation (Figure 5A). One of the clusters encoded the enzymes for catabolism of trimethylamine[39,40] (Tmm, trimethylamine monooxygenase and Tdm, trimethylamine *N*-oxide demethylase) and DMA[41] (DmmABC, DMA monooxygenase), while another cluster encoded the enzymes for catabolism of methylamine[42] (Gmas, γ-glutamylmethylamide synthetase; MgsABC, *N*-methylglutamate synthase; and MgdABCD, *N*-methylglutamate dehydrogenase). The transcriptome data showed that the transcription of *dmm*, *gmas*, *mgs*, and *mgd* genes was highly induced during the growth of strain NyZ550 on MET (Table S3), indicating that they encoded the enzymes responsible for the catabolism of DMA, a catabolic intermediate of MET. Moreover, assimilation of DMA in strain NyZ550 was most likely coupled to the serine cycle (Figure S12) due to the significant induction of its pathway genes and formate-tetrahydrofolate catabolic genes (Table S3).

Till date, the gene encoding the enzyme for hydrolysis of MET has not been identified. We analyzed the proteins encoded by the 107 upregulated genes in the InterPro protein families and domains database[43] to screen potential MET hydrolases. It turned out that a putative agmatinase was attractive due to its potential role in hydrolysis of the C−N bond. Agmatinase catalyzes the cleavage of the C−N bond of

https://doi.org/10.1021/acs.est.2c07669
Environ. Sci. Technol. 2023, 57, 1510−1519

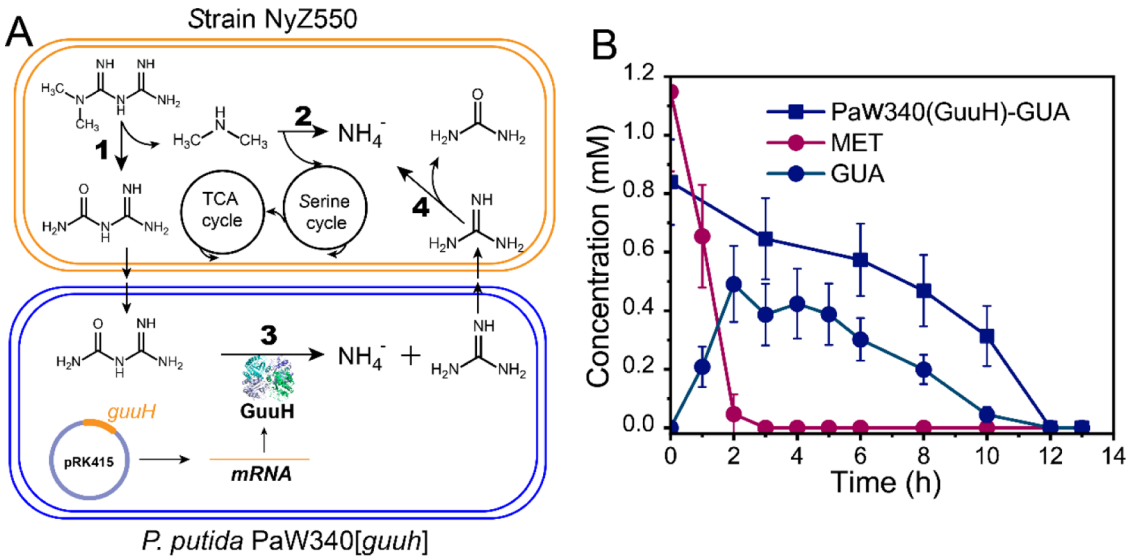

Figure 6. Complete degradation of MET and GUA by a synthetic co-culture. (A) Schematic diagram for the roles of the bacterial strains in the mixture. The key processes in MET and GUA degradation are shown: (1) hydrolysis of MET; (2) oxidative degradation of DMA; (3) hydrolysis of GUA; and (4) hydrolysis of guanidine. (B) Degradation of MET and GUA by the mixture.

agmatine with the formation of putrescine and urea. In this reaction, an oxygen atom from H_2O is incorporated into urea, which is similar to the reaction mechanism for hydrolysis of MET. Agmatinases are reported to be nickel or manganese-dependent hydrolase. Two genes encoding the nickel incorporation proteins (HypAB) which is required for the loading of divalent metal ion on agmatinase are adjacent to the upregulated agmatinase gene in strain NyZ550 (Figure 5A). Further investigations of MET hydrolase in biochemistry, catalytic mechanism, evolution, and ecological distribution would be helpful for a better understanding of the environmental fate of MET. Based on the metabolite analyses and results from transcriptomic sequencing, the degradation mechanism of MET and its intermediates by strain NyZ550 was inferred, as shown in Figure 5B.

GUA hydrolase was absent from the NyZ550 genome, which is consistent with the accumulation of GUA during degradation of MET. Although GUA was not degraded by strain NyZ550, guanidine, a known catabolic intermediate of GUA,[32] was readily utilized as a nitrogen source by strain NyZ550 (Figure 3B). A putative arginase of strain NyZ550 was homologous to the guanidinase GdmH (51% identity) from cyanobacterium *Synechocystis* sp. PCC 6803[44,45] likely catalyzed the conversion of guanidine into ammonium and urea.

3.8.2. Other Important Biological Processes Related to MET Degradation. MET is a hydrophilic compound and its degradation by strain NyZ550 is dependent on intracellular enzymes, and therefore, MET must be transported into the cell before it can be degraded. This process mainly involves energy metabolism, signal sensing, binding, and transmembrane transportation. As shown in Table S4, some bacterial chemotaxis genes were upregulated during growth on MET, which is beneficial for accessing and transporting substrates. Genes encoding ABC transporters and substrate-binding proteins were also upregulated, suggesting that they are likely involved in the transmembrane transportation of MET. Additionally, an upregulated gene encoding the putative guanidinium exporter is likely contributed to minimizing the stress exerted by exogenous MET or its catabolic products.

3.9. Degradation of MET and GUA by a Constructed Bacterial Mixture. Considering the risk of frequently detected GUA accumulation in the environment (Table 1)[22,24] and the accumulation of the dead-end product GUA in the degradation of MET by strain NyZ550 in this study, GUA degradation is also necessary for bioremediation of MET-contaminated sites. The results here regarding MET catabolism and the genes involved in strain NyZ550 clearly indicated that the conversion of GUA was the catabolic bottleneck. Thus, a bacterial mixture was constructed for complete degradation of MET and GUA, consisting of strain NyZ550 and *P. putida* PaW340 harboring a GUA hydrolase gene (*guuH*) (Figure 6A). GuuH converted GUA into guanidine,[32] which was subsequently utilized as a nitrogen source by strain NyZ550 (Figure 3B). *P. putida* PaW340 cells expressing GUA hydrolase (designated *P. putida* PaW340-[GuuH]) degraded GUA at a rate of 1.5 nmol mg protein^{-1} h^{-1} (Figure 6B). The bacterial mixture composed of strain NyZ550 and *P. putida* PaW340[GuuH] exhibited the capacity to eliminate both MET and GUA. MET (1.2 mM) disappeared within 3 h, accompanied by the significant accumulation of GUA with a maximum concentration of 0.5 mM at 2 h. Complete degradation of GUA was observed after 12 h (Figure 6B).

The constructed bacterial mixture capable of complete degradation of MET and GUA in water provides a potential strategy for bioremediation of MET-contaminated environments. The degradation of GUA appears to be the rate-limiting step for MET degradation in the environment, due to the fact that it is often detected as a dead-end product of MET. The results presented here suggest that the introduction of a GUA degrader can be a potential solution for accelerating complete removal of MET contamination through the combined effect of indigenous MET degraders in WWTPs, such as strain NyZ550.

3.10. Implications for MET-Contaminated Environments. Environmental exposure to MET is increasingly

https://doi.org/10.1021/acs.est.2c07669
Environ. Sci. Technol. 2023, 57, 1510−1519

recognized as an emerging issue threatening human health and ecological safety.[17,18,26,46] Clearly, microorganisms are the vital drivers of MET degradation in the environment. Here, based on an investigation of MET contamination in wastewater from WWTPs and the MET degradation capacity of microorganisms from these wastewater samples, we isolated and characterized a MET-degrading bacterium *Aminobacter* sp. strain NyZ550. Currently, the primary biodegradation pathways for MET are predicted based on identifying the MET metabolites in situ or derived from degradation by microbial consortia.[19,20] One of the possible degradation pathways involves the sequential removal of two urea, giving the first intermediate dimethylguanidine and subsequently DMA (Figure S6). Another conceivable pathway results in the production of biguanide through double dealkylation and further formation of GUA as a dead-end product[29] (Figure S6). Based on the results in this study and comparison with previously predicted pathways, a novel pathway for partial catabolism of MET in strain NyZ550 was proposed (Figure 5B). In this pathway, MET was directly hydrolyzed to produce GUA and DMA. Although GUA was not catabolized further, DMA was assimilated through a complete set of enzymes for methylamine degradation in strain NyZ550 (Figure 5), which is echoed by the fact that strain NyZ550 was able to grow on DMA, as shown in Figure 3A. The results support the observations of frequent accumulation of GUA in the environment[23,24] and suggest a possible role of this pathway in environmental transformation of MET. In the future, functional characterization of the catabolic enzymes involved in MET degradation at the genetic, biochemical, and ecological levels would broaden our understanding of the environmental fate of the widely used antidiabetic drug MET.

■ ASSOCIATED CONTENT

Supporting Information

The Supporting Information is available free of charge at https://pubs.acs.org/doi/10.1021/acs.est.2c07669.

Details of growth, biotransformation product identification, and transcriptome (PDF)

■ AUTHOR INFORMATION

Corresponding Author

Ning-Yi Zhou − *State Key Laboratory of Microbial Metabolism, Joint International Research Laboratory of Metabolic and Developmental Sciences, and School of Life Sciences and Biotechnology, Shanghai Jiao Tong University, 200240 Shanghai, China;* orcid.org/0000-0002-0917-5750; Email: ningyi.zhou@sjtu.edu.cn

Authors

Tao Li − *State Key Laboratory of Microbial Metabolism, Joint International Research Laboratory of Metabolic and Developmental Sciences, and School of Life Sciences and Biotechnology, Shanghai Jiao Tong University, 200240 Shanghai, China;* orcid.org/0000-0002-8255-7798

Zhi-Jing Xu − *State Key Laboratory of Microbial Metabolism, Joint International Research Laboratory of Metabolic and Developmental Sciences, and School of Life Sciences and Biotechnology, Shanghai Jiao Tong University, 200240 Shanghai, China*

Complete contact information is available at: https://pubs.acs.org/10.1021/acs.est.2c07669

Notes

The authors declare no competing financial interest.

■ ACKNOWLEDGMENTS

This work was funded by grants from the National Key R&D Program of China (2018YFA0901200) and the National Natural Science Foundation of China (NSFC) (32230001). We thank a number of colleagues for their help in collecting wastewater samples.

■ REFERENCES

(1) Orive, G.; Lertxundi, U.; Brodin, T.; Manning, P. Greening the pharmacy. *Science* **2022**, *377*, 259−260.

(2) Wilkinson, J. L.; Boxall, A. B. A.; Kolpin, D. W.; Leung, K. M. Y.; Lai, R. W. S.; Galbán-Malagón, C.; Adell, A. D.; Mondon, J.; Metian, M.; Marchant, R. A.; Bouzas-Monroy, A.; Cuni-Sanchez, A.; Coors, A.; Carriquiriborde, P.; Rojo, M.; Gordon, C.; Cara, M.; Moermond, M.; Luarte, T.; Petrosyan, V.; Perikhanyan, Y.; Mahon, C. S.; McGurk, C. J.; Hofmann, T.; Kormoker, T.; Iniguez, V.; Guzman-Otazo, J.; Tavares, J. L.; Gildasio De Figueiredo, F.; Razzolini, M. T. P.; Dougnon, V.; Gbaguidi, G.; Traoré, O.; Blais, J. M.; Kimpe, L. E.; Wong, M.; Wong, D.; Ntchantcho, R.; Pizarro, J.; Ying, G. G.; Chen, C. E.; Páez, M.; Martínez-Lara, J.; Otamonga, J. P.; Poté, J.; Ifo, S. A.; Wilson, P.; Echeverría-Sáenz, S.; Udikovic-Kolic, N.; Milakovic, M.; Fatta-Kassinos, D.; Ioannou-Ttofa, L.; Belušová, V.; Vymazal, J.; Cárdenas-Bustamante, M.; Kassa, B. A.; Garric, J.; Chaumot, A.; Gibba, P.; Kunchulia, I.; Seidensticker, S.; Lyberatos, G.; Halldórsson, H. P.; Melling, M.; Shashidhar, T.; Lamba, M.; Nastiti, A.; Supriatin, A.; Pourang, N.; Abedini, A.; Abdullah, O.; Gharbia, S. S.; Pilla, F.; Chefetz, B.; Topaz, T.; Yao, K. M.; Aubakirova, B.; Beisenova, R.; Olaka, L.; Mulu, J. K.; Chatanga, P.; Ntuli, V.; Blama, N. T.; Sherif, S.; Aris, A. Z.; Looi, L. J.; Niang, M.; Traore, S. T.; Oldenkamp, R.; Ogunbanwo, O.; Ashfaq, M.; Iqbal, M.; Abdeen, Z.; O'Dea, A.; Morales-Saldaña, J. M.; Custodio, M.; de la Cruz, H.; Navarrete, I.; Carvalho, F.; Gogra, A. B.; Koroma, B. M.; Cerkvenik-Flajs, V.; Gombač, M.; Thwala, M.; Choi, K.; Kang, H.; Ladu, J. L. C.; Rico, A.; Amerasinghe, P.; Sobek, A.; Horlitz, G.; Zenker, A. K.; King, A. C.; Jiang, J. J.; Kariuki, R.; Tumbo, M.; Tezel, U.; Onay, T. T.; Lejju, J. B.; Vystavna, Y.; Vergeles, Y.; Heinzen, H.; Pérez-Parada, A.; Sims, D. B.; Figy, M.; Good, D.; Teta, C. Pharmaceutical pollution of the world's rivers. *Proc. Natl. Acad. Sci. U.S.A.* **2022**, *119*, No. e2113947119.

(3) Kidd, K. A.; Blanchfield, P. J.; Mills, K. H.; Palace, V. P.; Evans, R. E.; Lazorchak, J. M.; Flick, R. W. Collapse of a fish population after exposure to a synthetic estrogen. *Proc. Natl. Acad. Sci. U.S.A.* **2007**, *104*, 8897−8901.

(4) Horký, P.; Grabic, R.; Grabicova, K.; Brooks, B. W.; Douda, K.; Slavik, O.; Hubena, P.; Santos, E. M. S.; Randak, T. Methamphetamine pollution elicits addiction in wild fish. *J. Exp. Biol.* **2021**, *224*, jeb242145.

(5) Sutherland, D. L.; Ralph, P. J. Microalgal bioremediation of emerging contaminants—Opportunities and challenges. *Water Res.* **2019**, *164*, 114921.

(6) International Diabetes Federation. In *IDF Diabetes Atlas*, 10th ed.: Brussels, Belgium, 2021.

(7) Patel, M.; Kumar, R.; Kishor, K.; Mlsna, T.; Pittman, C. U.; Mohan, D. Pharmaceuticals of emerging concern in aquatic systems: chemistry, occurrence, effects, and removal methods. *Chem. Rev.* **2019**, *119*, 3510−3673.

(8) Pentikäinen, P. J.; Neuvonen, P. J.; Penttila, A. Pharmacokinetics of metformin after intravenous and oral administration to man. *Eur. J. Clin. Pharmacol.* **1979**, *16*, 195−202.

(9) Tucker, G. T.; Casey, C.; Phillips, P. J.; Connor, H.; Ward, J. D.; Woods, H. F. Metformin kinetics in healthy subjects and in patients with diabetes mellitus. *Br. J. Clin. Pharmacol.* **1981**, *12*, 235−246.

(10) Oliveira, T. S.; Murphy, M.; Mendola, N.; Wong, V.; Carlson, D.; Waring, L. Characterization of pharmaceuticals and personal care products in hospital effluent and waste water influent/effluent by

direct-injection LC-MS-MS. *Sci. Total Environ.* **2015**, *518*−*519*, 459−478.
(11) Briones, R. M.; Sarmah, A. K.; Padhye, L. P. A global perspective on the use, occurrence, fate and effects of anti-diabetic drug metformin in natural and engineered ecosystems. *Environ. Pollut.* **2016**, *219*, 1007−1020.
(12) Tao, Y.; Chen, B.; Zhang, B. H.; Zhu, Z. J.; Cai, Q. Occurrence, impact, analysis and treatment of metformin and guanylurea in coastal aquatic environments of Canada, USA and Europe. *Adv. Mar. Biol.* **2018**, *81*, 23−58.
(13) Elizalde-Velázquez, G. A.; Gómez-Oliván, L. M. Occurrence, toxic effects and removal of metformin in the aquatic environments in the world: Recent trends and perspectives. *Sci. Total Environ.* **2020**, *702*, 134924.
(14) He, Y.; Zhang, Y.; Ju, F. Metformin contamination in global waters: Biotic and abiotic transformation, byproduct generation and toxicity, and evaluation as a pharmaceutical indicator. *Environ. Sci. Technol.* **2022**, *56*, 13528−13545.
(15) Lee, J. W.; Shin, Y. J.; Kim, H.; Kim, H.; Kim, J.; Min, S. A.; Kim, P.; Yu, S. D.; Park, K. Metformin-induced endocrine disruption and oxidative stress of Oryzias latipes on two-generational condition. *J. Hazard. Mater.* **2019**, *367*, 171−181.
(16) Crago, J.; Bui, C.; Grewal, S.; Schlenk, D. Age-dependent effects in fathead minnows from the anti-diabetic drug metformin. *Gen. Comp. Endocrinol.* **2016**, *232*, 185−190.
(17) Lin, W.; Yan, Y.; Ping, S.; Li, P.; Li, D.; Hu, J.; Liu, W.; Wen, X.; Ren, Y. Metformin-induced epigenetic toxicity in Zebrafish: Experimental and molecular dynamics simulation studies. *Environ. Sci. Technol.* **2021**, *55*, 1672−1681.
(18) Eggen, T.; Lillo, C. Antidiabetic II drug metformin in plants: uptake and translocation to edible parts of cereals, oily seeds, beans, tomato, squash, carrots, and potatoes. *J. Agric. Food Chem.* **2012**, *60*, 6929−6935.
(19) Trautwein, C.; Kümmerer, K. Incomplete aerobic degradation of the antidiabetic drug metformin and identification of the bacterial dead-end transformation product guanylurea. *Chemosphere* **2011**, *85*, 765−773.
(20) Markiewicz, M.; Jungnickel, C.; Stolte, S.; Białk-Bielińska, A.; Kumirska, J.; Mrozik, W. Primary degradation of antidiabetic drugs. *J. Hazard. Mater.* **2017**, *324*, 428−435.
(21) Armbruster, D.; Happel, O.; Scheurer, M.; Harms, K.; Schmidt, T. C.; Brauch, H. J. Emerging nitrogenous disinfection byproducts: Transformation of the antidiabetic drug metformin during chlorine disinfection of water. *Water Res.* **2015**, *79*, 104−118.
(22) Caldwell, D. J.; D'Aco, V.; Davidson, T.; Kappler, K.; Murray-Smith, R. J.; Owen, S. F.; Robinson, P. F.; Simon-Hettich, B.; Straub, J. O.; Tell, J. Environmental risk assessment of metformin and its transformation product guanylurea: II. Occurrence in surface waters of Europe and the United States and derivation of predicted no-effect concentrations. *Chemosphere* **2019**, *216*, 855−865.
(23) Scheurer, M.; Michel, A.; Brauch, H. J.; Ruck, W.; Sacher, F. Occurrence and fate of the antidiabetic drug metformin and its metabolite guanylurea in the environment and during drinking water treatment. *Water Res.* **2012**, *46*, 4790−4802.
(24) Trautwein, C.; Berset, J. D.; Wolschke, H.; Kümmerer, K. Occurrence of the antidiabetic drug metformin and its ultimate transformation product guanylurea in several compartments of the aquatic cycle. *Environ. Int.* **2014**, *70*, 203−212.
(25) Tisler, S.; Zwiener, C. Formation and occurrence of transformation products of metformin in wastewater and surface water. *Sci. Total Environ.* **2018**, *628*−*629*, 1121−1129.
(26) Zhang, R.; He, Y.; Yao, L.; Chen, J.; Zhu, S.; Rao, X.; Tang, P.; You, J.; Hua, G.; Zhang, L.; Ju, F.; Wu, L. Metformin chlorination byproducts in drinking water exhibit marked toxicities of a potential health concern. *Environ. Int.* **2021**, *146*, 106244.
(27) Mrozik, W.; Stefańska, J. Adsorption and biodegradation of antidiabetic pharmaceuticals in soils. *Chemosphere* **2014**, *95*, 281−288.
(28) Markiewicz, M.; Jungnickel, C.; Stolte, S.; Białk-Bielińska, A.; Kumirska, J.; Mrozik, W. Ultimate biodegradability and ecotoxicity of orally administered antidiabetic drugs. *J. Hazard. Mater.* **2017**, *333*, 154−161.
(29) Tisler, S.; Zwiener, C. Aerobic and anaerobic formation and biodegradation of guanylurea and other transformation products of metformin. *Water Res.* **2019**, *149*, 130−135.
(30) Briones, R. M.; Zhuang, W. Q.; Sarmah, A. K. Biodegradation of metformin and guanylurea by aerobic cultures enriched from sludge. *Environ. Pollut.* **2018**, *243*, 255−262.
(31) Poursat, B. A. J.; van Spanning, R. J. M.; Braster, M.; Helmus, R.; de Voogt, P.; Parsons, J. R. Biodegradation of metformin and its transformation product, guanylurea, by natural and exposed microbial communities. *Ecotoxicol. Environ. Saf.* **2019**, *182*, 109414.
(32) Tassoulas, L. J.; Robinson, A.; Martinez-Vaz, B.; Aukema, K. G.; Wackett, L. P. Filling in the gaps in metformin biodegradation: a new enzyme and a metabolic pathway for guanylurea. *Appl. Environ. Microbiol.* **2021**, *87*, e03003−e03020.
(33) Liu, H.; Wang, S. J.; Zhou, N. Y. A new isolate of Pseudomonas stutzeri that degrades 2-chloronitrobenzene. *Biotechnol. Lett.* **2005**, *27*, 275−278.
(34) Tiwari, D. K.; Jha, G.; Tiwari, M.; Kerkar, S.; Das, S.; Gobre, V. V. Synergistic antibacterial potential and cell surface topology study of carbon nanodots and tetracycline against E. coli. *Front. Bioeng. Biotechnol.* **2021**, *9*, 626276.
(35) Luo, R.; Liu, B.; Xie, Y.; Li, Z.; Huang, W.; Yuan, J.; He, G.; Chen, Y.; Pan, Q.; Liu, Y.; Tang, J.; Wu, G.; Zhang, H.; Shi, Y.; Liu, Y.; Yu, C.; Wang, B.; Lu, Y.; Han, C.; Cheung, D. W.; Yiu, S. M.; Peng, S.; Xiaoqian, Z.; Liu, G.; Liao, X.; Li, Y.; Yang, H.; Wang, J.; Lam, T. W.; Wang, J. SOAPdenovo2: an empirically improved memory-efficient short-read de novo assembler. *Gigascience* **2012**, *1*, 18.
(36) Iwasaki, K.; Uchiyama, H.; Yagi, O.; Kurabayashi, T.; Ishizuka, K.; Takamura, Y. Transformation of Pseudomonas putida by electroporation. *Biosci., Biotechnol., Biochem.* **1994**, *58*, 851−854.
(37) Du, E.; Terrer, C.; Pellegrini, A. F. A.; Ahlström, A.; van Lissa, C. J.; Zhao, X.; Xia, N.; Wu, X.; Jackson, R. B. Global patterns of terrestrial nitrogen and phosphorus limitation. *Nat. Geosci.* **2020**, *13*, 221−226.
(38) Artuso, I.; Turrini, P.; Pirolo, M.; Lugli, G. A.; Ventura, M.; Visca, P. Phylogenomic Reconstruction and metabolic potential of the genus Aminobacter. *Microorganisms* **2021**, *9*, 1332.
(39) Zhu, Y.; Jameson, E.; Parslow, R. A.; Lidbury, I.; Fu, T.; Dafforn, T. R.; Schäfer, H.; Chen, Y. Identification and characterization of trimethylamine N-oxide (TMAO) demethylase and TMAO permease in Methylocella silvestris BL2. *Environ. Microbiol.* **2014**, *16*, 3318−3330.
(40) Chen, Y.; Patel, N. A.; Crombie, A.; Scrivens, J. H.; Murrell, J. C. Bacterial flavin-containing monooxygenase is trimethylamine monooxygenase. *Proc. Natl. Acad. Sci. U.S.A.* **2011**, *108*, 17791−17796.
(41) Lidbury, I.; Mausz, M. A.; Scanlan, D. J.; Chen, Y. Identification of dimethylamine monooxygenase in marine bacteria reveals a metabolic bottleneck in the methylated amine degradation pathway. *ISME J.* **2017**, *11*, 1592−1601.
(42) Latypova, E.; Yang, S.; Wang, Y. S.; Wang, T.; Chavkin, T. A.; Hackett, M.; Schäfer, H.; Kalyuzhnaya, M. G. Genetics of the glutamate-mediated methylamine utilization pathway in the facultative methylotrophic beta-proteobacterium Methyloversatilis universalis FAM5. *Mol. Microbiol.* **2010**, *75*, 426−439.
(43) Blum, M.; Chang, H.-Y.; Chuguransky, S.; Grego, T.; Kandasaamy, S.; Mitchell, A.; Nuka, G.; Paysan-Lafosse, T.; Qureshi, M.; Raj, S.; Richardson, L.; Salazar, G. A.; Williams, L.; Bork, P.; Bridge, A.; Gough, J.; Haft, D. H.; Letunic, I.; Marchler-Bauer, A.; Mi, H.; Natale, D. A.; Necci, M.; Orengo, C. A.; Pandurangan, A. P.; Rivoire, C.; Sigrist, C. J. A.; Sillitoe, I.; Thanki, N.; Thomas, P. D.; Tosatto, S. C. E.; Wu, C. H.; Bateman, A.; Finn, R. D. The InterPro protein families and domains database: 20 years on. *Nucleic Acids Res.* **2020**, *49*, D344−D354.
(44) Wang, B.; Xu, Y.; Wang, X.; Yuan, J. S.; Johnson, C. H.; Young, J. D.; Yu, J. P. A guanidine-degrading enzyme controls genomic

https://doi.org/10.1021/acs.est.2c07669
Environ. Sci. Technol. 2023, 57, 1510−1519

stability of ethylene-producing cyanobacteria. *Nat. Commun.* **2021**, *12*, 5150.
(45) Funck, D.; Sinn, M.; Fleming, J. R.; Stanoppi, M.; Dietrich, J.; López-Igual, R.; Mayans, O.; Hartig, J. S. Discovery of a Ni^{2+}-dependent guanidine hydrolase in bacteria. *Nature* **2022**, *603*, 515−521.
(46) Wei, Z.; Wei, Y.; Li, H.; Shi, D.; Yang, D.; Yin, J.; Zhou, S.; Chen, T.; Li, J.; Jin, M. Emerging pollutant metformin in water promotes the development of multiple-antibiotic resistance in Escherichia coli via chromosome mutagenesis. *J. Hazard. Mater.* **2022**, *430*, 128474.

https://doi.org/10.1021/acs.est.2c07669
Environ. Sci. Technol. 2023, 57, 1510−1519